5

Recrystallization Behavior During Warm Compression of Martensite Steels

Pingguang Xu[1] and Yo Tomota[2]
[1]*Japan Atomic Energy Agency, Tokai, Ibaraki,*
[2]*Ibaraki University, Hitachi, Ibaraki,*
Japan

1. Introduction

The application of high strength-toughness-ductility structural steels is beneficial to reduce the body weight of automotives and to improve the usage efficiency of energy without any potential damage of safe and security of human beings. Grain refinement is an important fundamental research field for the development of such low alloy structural steels. The conventional thermo-mechanically controlled process (TMCP) of ferrite or ferrite-pearlite steels including severe deformation at a lower temperature of ferrite transformation and rapid cooling is usually utilized to refine the grain size down to about 5 microns. For ferrite/pearlite steels, the grain refinement through dynamic recrystallization was observed to take place at a true strain of 1.2 at 873K, and the fully recrystallized ferrite/cementite microstructure may be realized at a strain of 2.0 (Torizuka, 2005). The final grain size is dependent on the Zener-Hollomon parameter, *Z*, which is given by

$$Z = \dot{\varepsilon} \cdot \exp(\frac{Q}{RT}) \tag{1}$$

where $\dot{\varepsilon}$, Q, R and T refer to the strain rate, the activation energy, the gas constant, and the absolute temperature, respectively. Because the severe deformation in uni-directional rolling cannot meet the requirement on Z-value for full recrystallization, the multi-directional groove rooling process has been developed recently. Unfortunately, the groove rolling process is unsuitable to the commercial production of wide steel plates.

In various microstructure types, the martensite was expected to have a low critical strain requirement for grain refinement because the high density dislocations, the supersaturated solute carbon and the ultrafine laths are helpful to raise the stored energy. The advantage of martensite was firstly claimed (Miller, 1972) as an initial microstructure to obtain ultrafine ferrite-austenite microstructures through cold-rolling and annealing of Ni(-Mn)-C martensite steels. The cold rolling and annealing of lath-martensite was confirmed (Ameyama, 1988) much effective to make ultrafine grained microstructures of low carbon steels. Ueji et al (2002) have claimed that the formation of ultrafine grained microstructure by cold rolling followed by annealing is closely related to the fine substructures and the high density dislocations of martensite. However, the cold rolling of martensite steel requires much higher loading capacity of mills and the microcracks may occur in the surface layers and/or the side edges of martensite steel plates.

Hayashi *et al* (1999, 2002) reported that the multi-pass warm groove-rolling of low-carbon martensite could produce an ultrafine ferrite-cementite microstructure less than 1μm. Tomota *et al* proposed to realize the grain refinement by warm compression or warm rolling of martensite steel plates through the dynamic recrystallization and confirmed that the dynamic recrystallization occurs at a low critical strain during warm compression for martensite of a low-carbon SM490 steel (Bao, 2005a). This technique has been successfully employed to get ultrafine grained ferrite-cementite microstructure (Li, 2008) and ultrafine grained ferrite-austenite microstructure (Xu, 2008a). Furuhara *et al* (2007) found that an initial microstructure of high carbon martensite is preferable to reduce the critical strain for full dynamic recrystallization, showing that the cementite particles can act as hard particles to promote the dynamic recrystallization during the martensite warm deformation. Though the carbon enriched retained austenite usually transforms to martensite to improve ductility, its detailed role during warm compression was necessary to be clarified. Therefore, the neutron diffraction was applied to *in situ* investigate the precipitation of austenite and the recrystallization of ferrite in 17Ni-0.2C martensite steel during warm compression. The existence of carbon enriched austenite particles during warm compression was found to further promote the dynamic recrystallization of ferrite from lath martensite by playing a role of the hard second phase (Xu, 2008b).

In this chapter, the research progress in dynamic recrystallization and grain refinement during warm compression of martensite steels was reviewed systematically while the advantages of *in situ* neutron diffraction were emphasized as a powerful beam technique suitable for clarifying the microstructure evolution during various thermo-mechanically controlled processes.

2. Dynamic recrystallization during warm compression in low alloy martensite steel

The dynamic recrystallization is one of the effective ways to refine microstructure to improve strength-toughness balance. Torizuka *et al* (2005) carried out a systematic study on warm compression and warm rolling for a conventional low-carbon ferrite/pearlite steel, realized a submicron ferrite-cementite microstructure through continuous dynamic recrystallization during heavy deformation up to a true strain of 3~4 and successfully produced the ultrafined grained high strength wires, rods and even steel plates with 300mm in width. However, it is difficult to apply such severe deformation with a high Z-value to commercial production of wider plates or sheets.

The average grain size of dynamically recrystallized microstructure was found to be dependent on Z-value and independent on the initial micrsotructure type such as ferrite or ferrite-pearlite or martensite (Ohmori, 2002; Ohmori, 2004; Bao, 2005a; Bao, 2005b). Though the initial grain size and the compressive strain in cases of ferrite or ferrite-pearlite initial microstructure have no direct effect on the average grain size of final ferrite microstructure, it is not clear about the effects of initial austenite grain size, strain and pre-tempering treatment on the dynamic recrystallization and the final grain size during the warm compression of martensite. Li *et al* (2008) investigated the effects of initial microstructure, deformation strain and pre-tempering on dynamic recrystallization of ferrite from lath martensite by using a commercial low-carbon steel, JIS/SM490 (mass%: 0.16C-1.43Mn-

0.41Si-0.014P-0.004S-0.01Cu-0.027Al-0.028N). The transformation temperatures measured by dilatometry at a heating and cooling speed of 5K/s were 1010K for Ac1, 1133K for Ac3 and 895K for Ar1, respectively (Bao, 2005a). Cylindrical compressive specimens with ϕ4mm×6mm were spark cut from the 15×15mm martensite steel bars obtained by water quenching after solid solution treatment at 1273K for 3.6ks. The specimens were heated up to 873K or 923K, held there for 1s, compressed by true strain ε = 0.3, 0.55 or 0.7 at 1.7×10^{-3} s^{-1}, and then quenched into water. Some specimens were pre-tempered at 873K or 923K for 3.6ks before the warm compression. The deformed specimens were cut along the longitudinal direction and the central area of the sectioned plane was observed with a field emission scanning electronic microscope (FE-SEM).

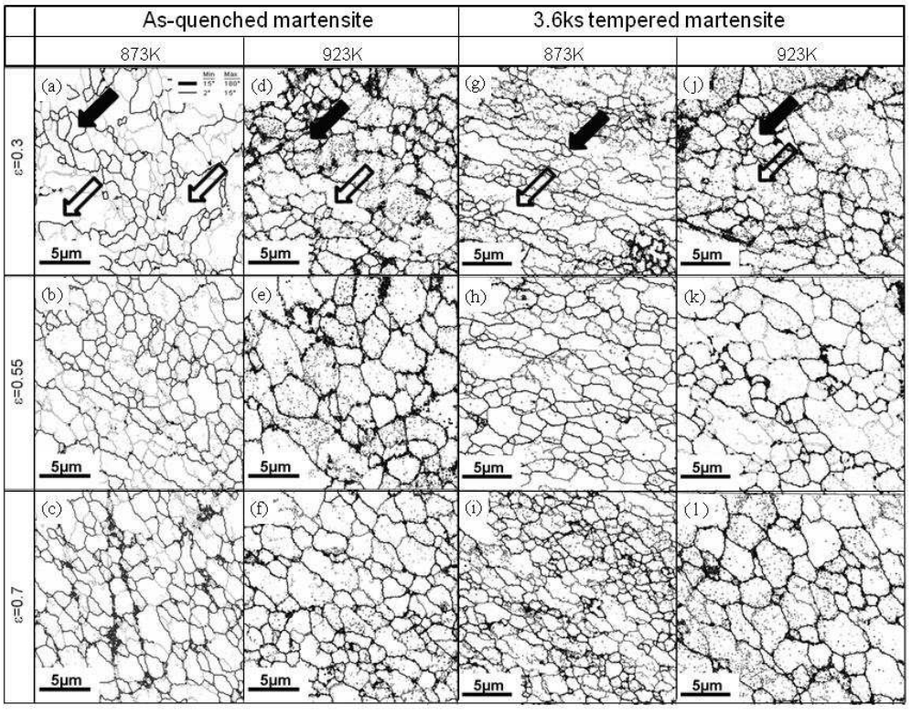

Fig. 1. Boundary misorientation mappings for the specimens deformed at 1.7×10^{-3} s^{-1} where the initial martensite was quenched from 1273K.

Fig.1 summarized the boundary misorientation mappings for the specimens warm compressed at 1.7×10^{-3} s^{-1}, where the solid arrows marked the recrystallized ferrite grains surrounded only by high angle grain boundaries (here called as Type I grains, according to Torizuka's definition (2005)) and the open arrows marked the recrystallized ferrite surrounded partially by high angle boundaries (here called as Type II grains). The Type I grains can be observed after the true strain 0.3 in all cases, revealing much lower critical strain for the initiation of dynamic recrystallization of low carbon martensite microstructure. This is surprizingly low because the critical strain is higher than 1.0 for the conventional ferrite-pearlite initial microstructure (Torizuka, 2005). The Type II grains equaxilize gradually and its size becomes almost equal to that of Type I grains with increasing of strain. It is also found that the grain size of Type I grains at a lower temperature (873K) deformation is smaller than that at a higher temperature (923K), revealing that the grain size

is dependent on the Z-value. Moreover, compared with (c) and (i), it can be found that the 3.6ks prior tempering at 873K leads to the increase of Type I grains and smaller Type II grains, suggesting the prior tempering promote the dyanmic recrystallization. However, compared with (f) and (l), the 3.6ks prior tempering at 923K does not acclerate the grain refinement process. The observation of initial micorstructure before warm compression shows that the pretempering at 873K enables the dispersive precipitation of cementite particles and the dislocationes in martensite do not disappear so much, while the pretempering at 923K reduces the dislocation density and increases the size of cementite particles (Li, 2008). Consequently, the acceleration of dynamic recrystallization after the lower temperature pre-tempering (873K) is mostly related to the dispersive precipitation of cementite particles, while the delay of dynamic recrystallization after the higher tempatrue pretempering (923K) is mostly related to the decrease in dislocation density.

3. Dynamic recrystallization and austenite precipitation during warm compression in high nickel martensite steels

While the submicron ultrafine grained ferrite/cementite microstructure shows the limited ductility, the submicron ultrafine grained austenite/ferrite duplex microstructure possesses up to 1000MPa tensile strength and 25% uniform elongation (Tomota, 2008). Because the austenite can evidently improve the tensile ductility through the transformation induced plasticity (TRIP) effect, it leads to higher possibility for industrial applications. As mentioned in Section 1, warm compression or rolling of martensite microstructure with initial fine substructures and the high density dislocations of martensite can be utilized to accelerate the recrystallization and refine grains at a low critical strain (Bao, 2005a and 2005b). It was suspected that the competition of austenite precipitation and ferrite recrystallization played an important role to obtain ultrafine grained structures (Enomoto, 1977). However, the effects of austenite amount and its thermomechanical stability related to carbon concentration on the dynamic recrystallization of ferrite and the formation of ultrafine grain microsructure have not been clarified (Maki, 2001).

Xu et al investigated the effects of austenite precipitation and the carbon enrichment in austenite on the dynamic recrystallization during warm compression by using 18Ni and 17Ni-0.2C (mass%) martensite steels (Xu, 2008a) where 843K and 773K were chosen as the pre-tempering temperature according to the phase diagrams of Fe-Ni and Fe-Ni-C alloys, respectively. Cylindrical samples with 6.5 mm in length and 4mm in diameter for compression tests were prepared by spark cutting and surface grinding. The samples were heated up to the deformation temperature at a heating rate of 5K/s and then deformed at 8.3×10^{-4}/s followed by water quenching. The longitudinally sectioned specimens were electrochemically polished to avoid the stress-induced martensite transformation of austenite.

3.1 SEM microstructure observation and EBSD microstructure characterization

Fig.2 showed the different pre-tempered 17Ni-0.2C microstructures before and after warm compression at 773K. Different from the non-tempered martensite (Fig. 2(a)), small particles can be found in the tempered martensite matrix (marked by circle in Fig. 2(b)), and these particles are coarser (marked by circle in Fig.2(c)) after long-time pre-tempering. In the specimen warm

compressed without any pre-tempering, ultrafine equiaxed grains (marked by white arrow) predominate the SEM microstructure while some elongated grains (marked by gray arrow) related to recovery can be also found. In contrast, the warm deformed specimen with 3.6ks pre-tempering shows a fully equiaxed microstructure, and the ferrite grains are much finer. However, the warm compression after 36ks pre-tempering results in a partially equiaxed microstructure, revealing the long-time pre-tempering retards the ferrite recrystallization evidently and a larger compressive strain is necessary to achieve full recrystallization.

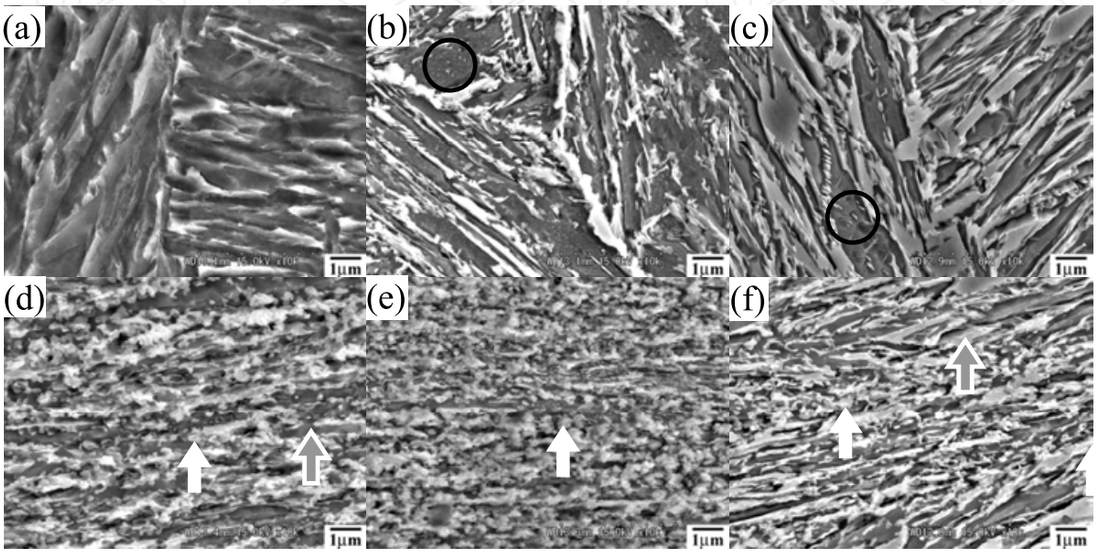

Fig. 2. SEM microstructures of 17Ni-0.2C steels before (a, b and c) and after (d, e and f) warm compression at 773K, ε=0.6, 8.3×10^{-4}/s. (a, d) non-tempered; (b, e) 3.6ks tempered; (c, f) 36.0ks tempered. The compression axis is along the vertical direction. (Xu, 2008a)

Fig.3 showed the electron back-scattering diffraction (EBSD) maps of 18Ni steel microstructures before and after warm deformation, where the compression axis is along the vertical direction. The volume fraction of the retained austenite amount in the non-tempered microstructure is less than 1%, and increases hardly after the 3.6ks pre-tempering.

In the ε=0.6 warm compressed specimen without pre-tempering, the equiaxed ferrite grains are dominative although many grains are still with small misorientation; in case of 3.6ks pre-tempering, the equiaxed ferrite grains are much few and the average grain size is a little coarser, suggesting that the decrease in dislocation density in the initial microstructure by pre-tempering brings clearly negative influence on the dynamic recrystallization.

After a larger strain warm compression (ε=0.8), the fully equiaxed ferrite grains can be obtained in both cases and their average grain sizes are approximately equal. Although blocky austenite grains are not observed in the microstructures after warm compression, the local regions with a confidence index of less than 0.2 (marked by circles) are related to the metastable austenite at high temperature, partially transformed to martensite /austenite islands during rapid cooling to room temperature for the sample preparation. Considering that such conventional microstrure quenching(freezing) process is not so ideable, the *in situ* microstructure evaluation involving neutron diffraction (see Section 4) is much important for investigation on the high temperature microstructure evolution.

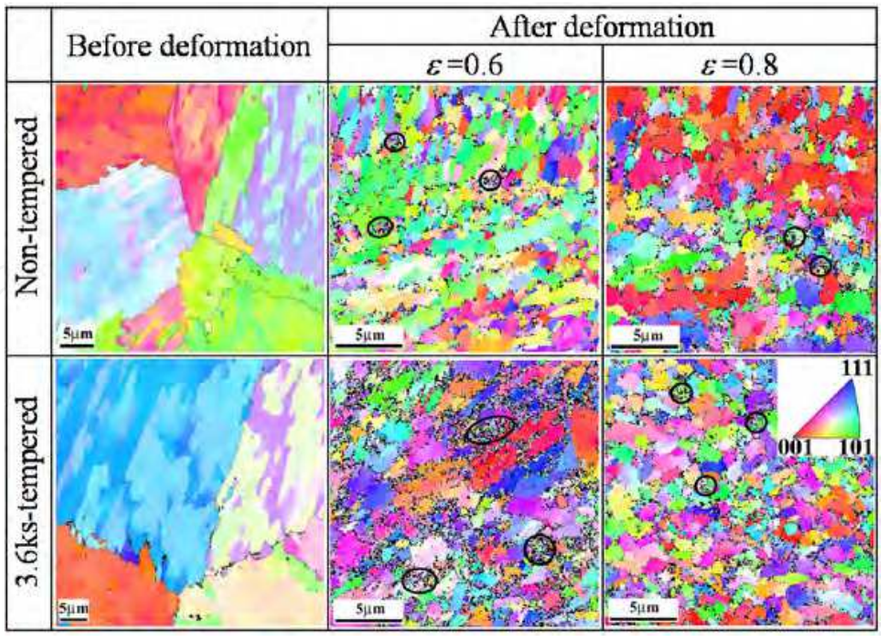

Fig. 3. Crystallographic orientation characteristics of 18Ni martensite steel before and after warm compression at 843K, 8.3×10^{-4}/s. (Xu, 2008a).

Fig.4 gives the EBSD maps of 17Ni-0.2C microstructures before and after warm compression. The austenite volume fraction is plotted in Fig.5. For the non-tempered specimen, the austenite amount increases much after deformation (from 9.5% to 17%) and its average grain size of austenite decreases evidently because of the precipitation of ultrafine grained austenite during warm deformation. After warm deformation, the equiaxed ferrite grains in the local regions with bulky austenite (marked by circle) are with large misorientation but those in the regions with no bulky austenite (marked by reactangle box) are with small misorientation, showing that the ferrite dynamic recrystallization is related to the existence of bulky austenite grains.

The 3.6ks pre-tempering leads to an clear increase of austenite amount. After the ε=0.6 warm compression, the ferrite-austenite duplex microstructure becomes fully equiaxed and the volume fraction of austenite increases from 18% before deformation to 36.8% after deformation and the average size of austenite grains decreases from 1.53μm before deformation to 0.94μm after deformation, which also proves that the warm deformation promotes the precipitation of ultrafine grained austenite. Meanwhile, the ferrite grains are refined to 0.85μm after deformation, smaller than that of 3.6ks pre-tempered 18Ni steel after warm compression at a strain of 0.8. It reveals that the higher Z-value (17Ni-0.2C, 773K, $Z=1.21\times10^{14}$ s^{-1}; 18Ni, 843K, $Z=4.55\times10^{12}$ s^{-1}) and the high carbon content are helpful to refine the fully recrystallized microstructure.

When the pre-tempering time prolongs to 36.0ks, the austenite amount approaches 33.8% after the isothermal tempering treatment. After the ε=0.6 warm deformation, the ferrite grains are elongated and coarse, showing that the dynamic recrystallization is delayed evidently. Meanwhile, the austenite amount measured at room temperature decreases abruptly to 13.8%. According to the phase diagram, the equilibrium microstructure at

773K consists of ferrite, austenite and cementite. The austenite amount after long-time pre-tempering in Fig.5 increases evidently due to the austenite precipitation at an elevated temperature below the martensite reverse transformation starting temperature, which is consistent with the previous reports for a Fe-Ni martensite alloy (Enomoto, 1977) and for a 18Ni-12Co-4Mo maraging steel (Moriyama, 2001). The decreasing austenite amount after warm compression is related to the weakening of austenite thermal stability caused by the carbon depletion in austenite after cementite precipitation. Since the cementite particles are mostly in nanometer scales, TEM observations are necessary.

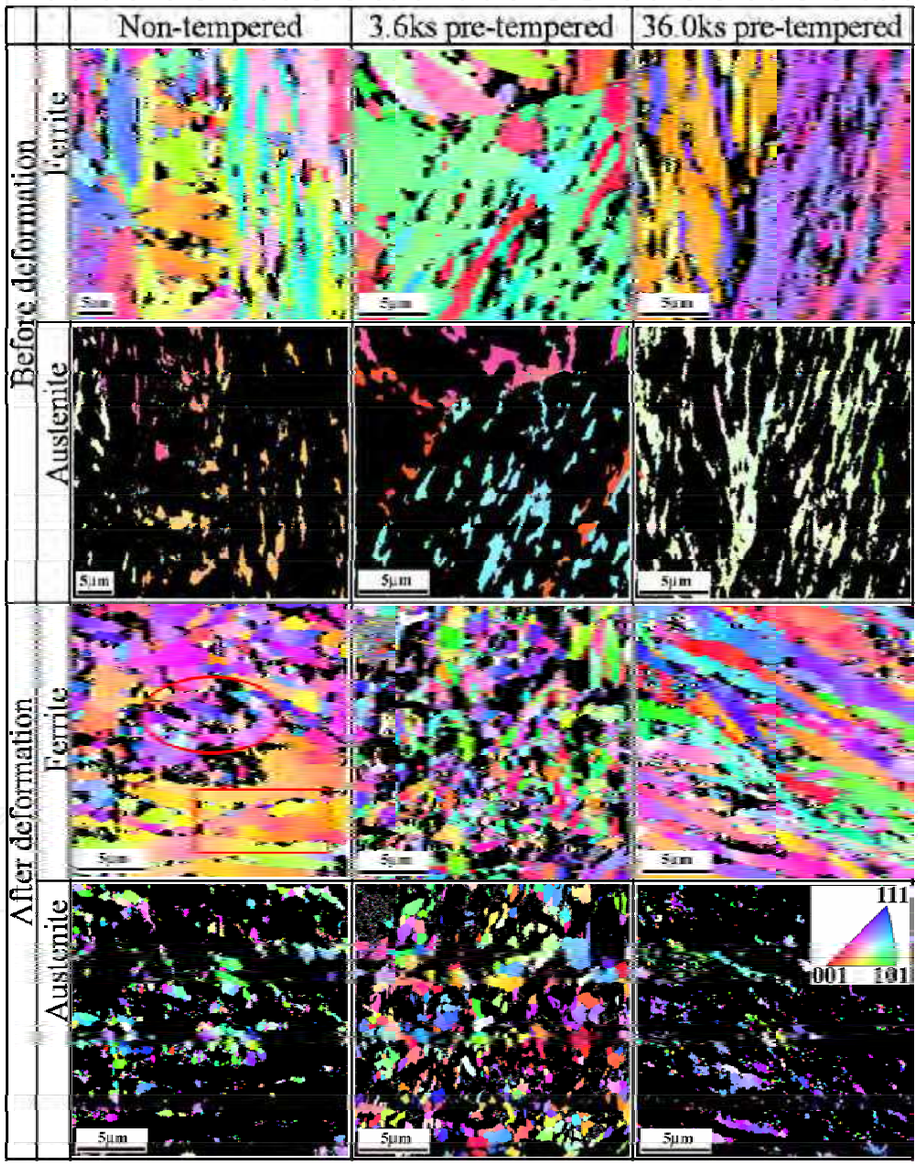

Fig. 4. Crystallographic orientation characteristics of different pre-tempered 17Ni-0.2C martensite steel specimens before and after warm compression at 773K, 8.3×10^{-4}/s. The compression axis is along the vertical direction (Xu, 2008a).

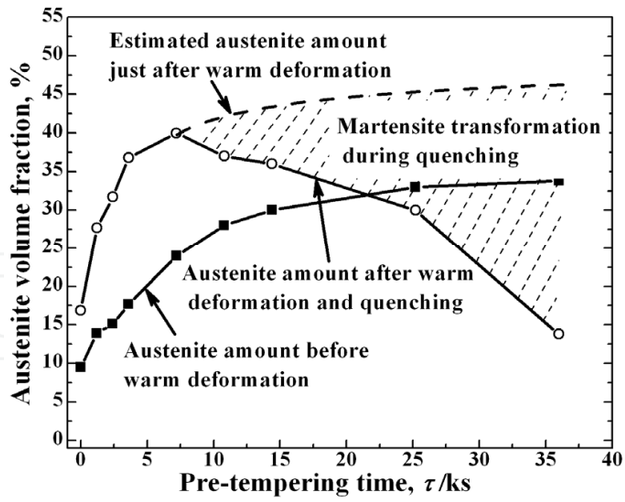

Fig. 5. Change in the austenite amount of 17Ni-0.2C steel by pre-tempering and warm deformation at 773K according to EBSD phase mapping statistics (Xu, 2008a).

3.2 TEM microstructure observation and EDX composition analysis

Fig.6 shows the bright field images for the non-tempered (a) and pre-tempered (b, c) microstructures of 17Ni-0.2C steel after warm compression. In the case of no pre-tempered condition, large ferrite grains near the austenite particles can be found with high density dislocations and some new grains with no intragranular dislocations form in these regions. It is found in Fig. 6(a) that the high angle grain boundaries surrounded an individual ferrite grain. In the warm compressed specimen after 3.6ks pre-tempering, the ultrafine equiaxed ferrite and austenite grains can be found frequently (Fig. 6(b)), suggesting that the warm deformation promotes the austenite precipitation and the ferrite dynamic recrystallization. The misorientation analysis confirms that the grain boundaries between these grains and their neighbors are of high angle boundaries, exhibiting that the dynamic recrystallization of ferrite can be confirmed really to take place during the warm deformation.

In case of the 36ks tempering, the elongated martensite laths within low dislocation density are clearly observed, which is related to the recovery of martensite. It is also found that the cementite precipitates preferably around the carbon-enriched austenite grains located at the martensite lath boundaries rather than within the martensite laths. The warm deformation accelerates the carbon diffusion and promotes the dynamic precipitation of spherical cementite particles within the martensite laths (Fig.6(c)).

For a pre-tempering time longer than 7.2ks, the carbon partitioning from martensite to austenite is gradually replaced by the cementite precipitation. Because of the precipitation of cementite particles and the increase of austenite amount, the average carbon concentration in austenite must decrease, finally lower than that in the 3.6ks tempered and deformed specimen. As a result, the thermal stability of austenite decreases, some austenite grains transform to martensite upon cooling after deformation and the fresh nanometer-scale martensite particles form around the cementite and austenite particle (Fig.6(c)). Hence the austenite amount after rapid cooling to room temperature becomes smaller (see Fig.4). The low density dislocations and no carbon-enriched austenite lead to the delayed dynamic

recrystallization in the 36ks pre-tempered and warm compressed specimen when compared with the 3.6ks pre-tempered and warm compressed specimen.

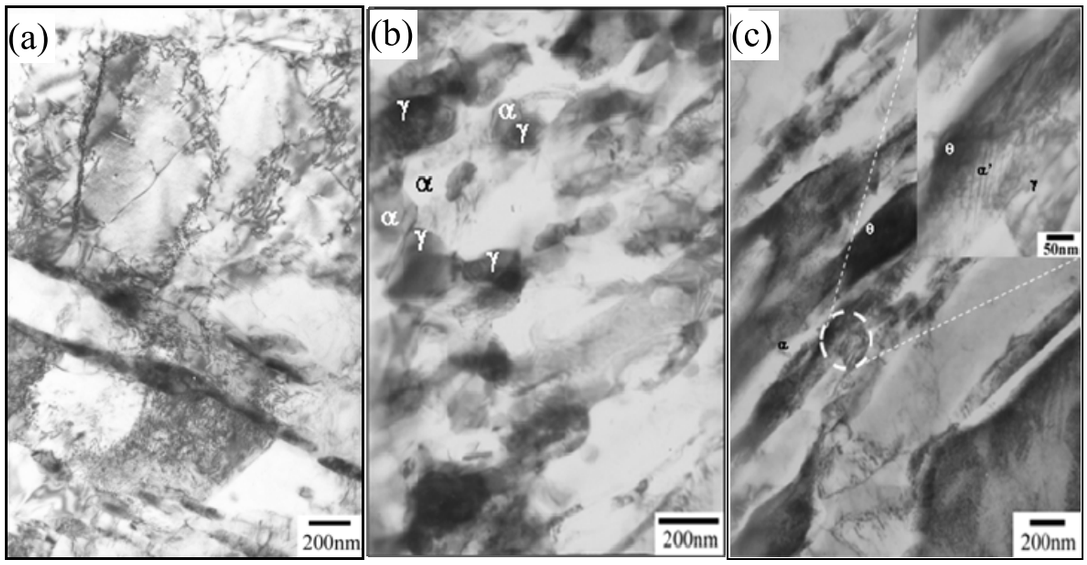

Fig. 6. Transmission electron microscopic microstructures of different pre-tempered 17Ni-0.2C steel after warm compression at 773K, $8.3x10^{-4}$ /s: (a) non-tempered; (b) 3.6ks pre-tempered; (c) 36ks pre-tempered.

According to the Fe-Ni and Fe-Ni-0.2C equilibrium phase diagrams, the nickel-rich austenite should appear at 843K in 18Ni and the nickel-rich and carbon-rich austenite and cementite should appear at 773K in 17Ni-0.2C. The EDX composition analysis proves that the metastable austenite (or martensite) is nickel-enriched, for example, the nickel content is about 20-26mass% (austenite) versus 15-16mass% (ferrite) in 17Ni-0.2C. Though the EDX analysis can not provide a reliable carbon concentration in constituent phases, the austenite in the 3.6ks pre-tempered 17Ni-0.2C after warm compression should be carbon-eniriched because (a) no cementite particles are found in such microstructure, (b) the stability of austenite phase is much higher than that in 18Ni, (c) the diffusion of carbon is more rapid than that of nickel and (d) the interstitial solubility of carbon is much higher in austenite than in ferrite. Considering that the 3.6ks pre-tempering decreases the dislocation density of martensite substructures, the accelerate dyamic recrystallization is mainly related to the formation of a large amount of carbon-enriched austenite.

3.3 Effect of carbon-enriched austenite on dynamic ferrite recrystallization

Generally, the retained austenite at room temperture is softer than the corresponding martensite. If there is no *in situ* quantitative micromechanical data of two duplex microstructure at elevated temperature, it will be much difficult to clarify why the existence of carbon-enriched austenite promotes the dynamic ferrite recrystallization during warm compression. Fortunately, the *in situ* neutron diffraction study about 3.6ks pre-tempered 17Ni-0.2C steel (Xu, 2008b) showed that the heterogeneous deformation occurs during warm compression at 773K and the ferrite matrix is subject to larger plastic deformation than the carbon-enriched austenite, i.e. the former is softer than the latter. Moreover, it was

found that before and after approaching the critital strain ε=0.13, the ferrite (hkl) reflections showed clear difference among their relative integrated intensities because of the occurrence of dynamic ferrite recrystallization. In addition, the splitting of austenite reflection peaks and its disappearance during warm compression obtained by a neutron diffraction study (Xu, 2008b) help us to understand the change in carbon concentration of austenite during the warm compression. Consequently, the influencing mechanism of carbon-enriched austenite on the heterogeneous deformation and the ferrite-austenite duplex microstructure evolution can be summarized as shown in Fig.7.

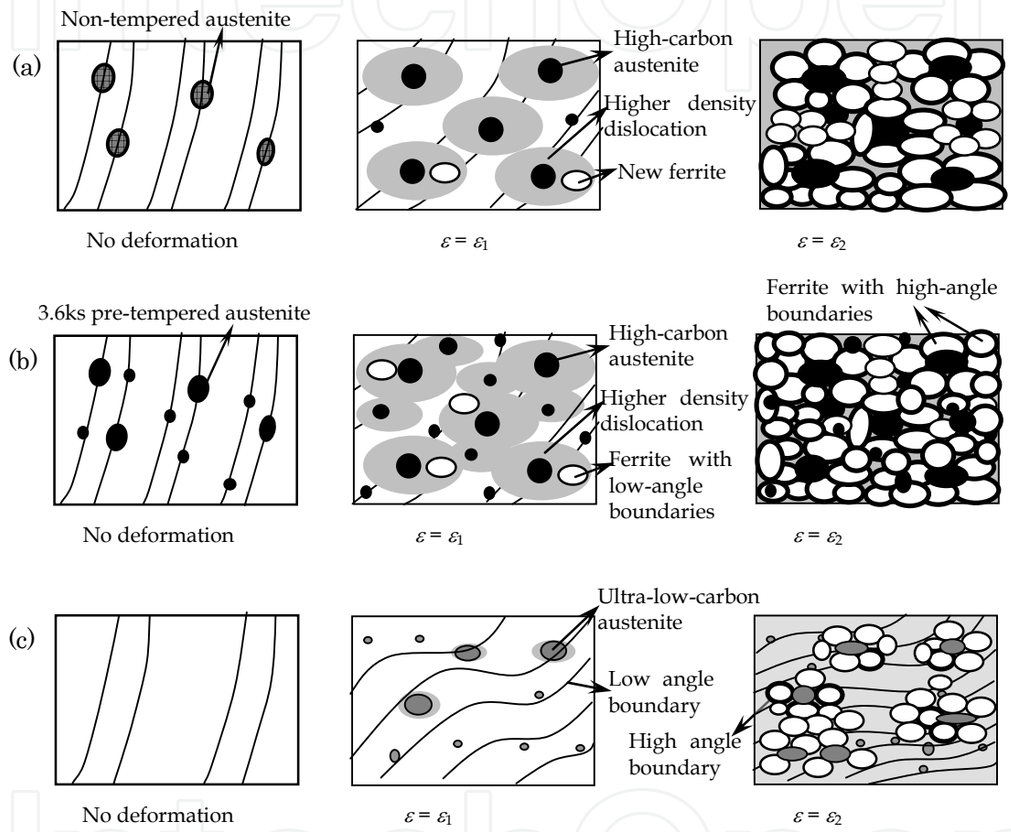

Fig. 7. Schematic illustration for microstructure evolution of martensite steels with different carbon contents during warm deformation, where the compression axis is along the vertical direction and $\varepsilon_1<\varepsilon_2$: (a) 17Ni-0.2C, non-tempered, at 773K; (b) 17Ni-0.2C, 3.6ks pre-tempered, at 773K; (c) 18Ni, at 843K. (Xu, 2008a)

For the carbon-added high-nickel steel, the amount of carbon-enriched austenite increases due to the proper pre-tempering and the austenite particles becomes harder than the pre-tempered martensite (or recovered ferrite matrix) during warm compression. Hence the larger local plastic flow takes place in the regions around austenite particles. When the local plastic strain increases to a critical value ($\varepsilon=\varepsilon_1$), the recrystallized ferrite grains preferably nucleate in these local regions near the austenite particles according to the related recrystallization model (Doherty, 1997). When the true strain increases to another critical value ($\varepsilon=\varepsilon_2$), all the ferrite grains are equiaxed and fully recrystallized (Fig. 7(b)).

In case of no pre-tempering, the austenite amount is relatively less than that in case of 3.6ks pre-tempering and the carbon content in austenite is lower than that in the latter. Although the warm compression promotes the austenite precipitation and the carbon enrichment in austenite, the plastic deformation partitioning between austenite particles and recovered ferrite matrix is a little weaker. Consequently, at the true strains $\varepsilon=\varepsilon_2$, the recrystallized ferrite amount is correspondingly less than that in the case of 3.6ks pre-tempering (Fig. 7(a)).

When the pre-tempering time is extended to more than 14.4ks, the precipitation of cementite particles leads to relative carbon depletion in austenite, and the plastic deformation partitioning between the austenite and the recovered ferrite matrix is no longer apparent. Hence the dynamic recrystallization of ferrite is retarded markedly (Maki, 2001). The coarse austenite grains formed during long-time pre-tempering are metastable because of low carbon concentration, easy to deform during warm compression, and then transform to martensite (or ferrite matrix) upon rapid cooling to room temperature.

For the ultra-low-carbon high-nickel steel, the plastic deformation partitioning is relatively weak since the carbon-enriched austenite is impossible to form and martensite is easy to recover. Moreover, the dislocation density in the martensite matrix is lower than that in carbon-added high-nickel steel and the block is also coarser. As a result, a larger compressive strain is needed for the full recrystallization (Fig. 7(c)).

As a summary, the following conclusions should be mentioned. The carbon addition is beneficial to reduce the critical strain for full recrystallization of high-nickel martensite steels during warm compression. The increment of carbon-enriched austenite volume fraction accelerates the dynamic recrystallization of ferrite through plastic deformation partitioning in the 17Ni-0.2C steel. Proper pre-tempering promotes the precipitation of the carbon- and nickel-enriched austenite, and then promotes the dynamic recrystallization in the 17Ni-0.2C steel. On the other hand, long-time tempering leads to the carbon depletion in austenite so as to delay the dynamic recrystallization. In the 18Ni steel, a larger warm compression strain is required for full recrystallization during warm compression, mainly because of no carbon-enriched austenite.

4. Dynamic microstructure evolution in high nickel martensitic steel during warm compression studied by *in situ* neutron diffraction

As mentioned in above sections, a large strain and a high Zener-Hollomon value may be unnecessary to obtain ultrafine grained microstructures if the martensite initial microstructure is employed during annealing after cold working (Miller, 1972; Ameyama, 1988) or during warm deformation (Hayashi, 1999, Bao, 2005a). The microstructural observation of warm compressed specimens with different amounts of pre-existing austenite has shown that a dynamically recrystallized microstructure can be obtained in a 17Ni-0.2C martensite steel at a small strain ($\varepsilon \leq 0.6$). In order to make clear the microstructure evoluton and to investigate the effect of the austenite particles on dynamic recrystallization, the *in situ* Time-Of-Flight (TOF) neutron diffraction for the as-quenched 17Ni-0.2C steel during warm compression was carried out using the ENGIN-X neutron diffractometer at ISIS, Rutherford Appleton Laboratory.

Since the warm deformation at a temperature just below the austenite transformation starting temperature accelerated the austenite transformation significantly, a little low temperature (773K) was selected in order to investigate the dynamic recrystallization of ferrite. Here, 3.6ks pre-tempering treatment at 773K was carried out to obtain about 18vol% austenite in the initial microstructure. Cylinder specimens with 8mm diameter and 20mm length were prepared by spark cutting and surface grinding.

A 100kN hydraulic loading rig attached with a radiant furnace with a control error of ±1K was employed to realize the thermomechanically controlled process (TMCP). The specimen was heated up to 773K and neutron diffraction spectrum during the isothermal holding was collected repeatedly with 1min acquisition time to investigate the effect of the tempering process on the microstructure evolution. After 600s isothermal holding at 773K, the specimen was compressed at a strain rate of 8.3×10^{-4} s^{-1} and the neutron diffraction spectra were acquired at 773K. In order to decrease the experimental error, each neutron spectrum was summed with the consecutive one for the purpose of applying the Rietveld refinement.

Because it was difficult to distinguish the diffraction peaks of ferrite and martensite using the relative weak neutron spectra, the tempered/deformed martensite and the recrystallized ferrite during warm compression are here simply designated as the ferrite matrix. The austenite volume fraction was determined by the Rietveld refinement using the General Structure Analysis System (GSAS) software package (Larson, 2004), taking all diffraction peaks measured into consideration. The texture indexes (Bunge, 1982) of warm deformed austenite and ferrite were evaluated by the spherical harmonic preferential orientation fitting with an assumption of cylindrical sample symmetry, and the series was truncated at a maximum expansion order of l_{max}=8. Single peak fitting with the third TOF profile function (Larson, 2004) was employed to obtain the integrated intensities and the lattice spacings of (*hkl*) peaks. The preferred orientations and the lattice strains of ferrite and austenite were also analyzed by these integrated intensities and lattice spacings, respectively.

4.1 Microstructure evolution during isothermal holding

Fig.8 gives the axial neutron spectrum acquired in 600s at room temperature and the corresponding Rietveld refinement result where the small residual error reveals that the profile fitting quality is good enough. The austenite amount of the 3.6ks pre-tempered 17Ni-0.2C martensite steel is about 21.0±0.3%, a little higher than that measured by EBSD technique for an electrochemically polished sample (about 18%), which is possibly related to the weak stability of austenite, *i.e.* martensite transformation near surface (Chen, 2006). Actually, the neutron diffraction, as an important materials characterization technique different from the X-ray and electronic diffraction, enables to measure a large sample with a large gauge volume and to get bulk average information with high statistics and to evaluate the microstructure evolution under various environments, especially for multiphase materials.

Fig.9 shows the change in austenite mass fraction during isothermal holding at 773K. The austenite amount increases slowly and results in about 1.5% increment after 600sec isothermal holding. This precipitation speed is consistent with that estimated by the microstructure observation where the austenite amount increases from 9.5% before tempering to about 18% after 60min tempering at 773K (Xu, 2008a). These results also reveal

that the neutron diffraction technique is suitable to evaluate the austenite precipitation during isothermal holding.

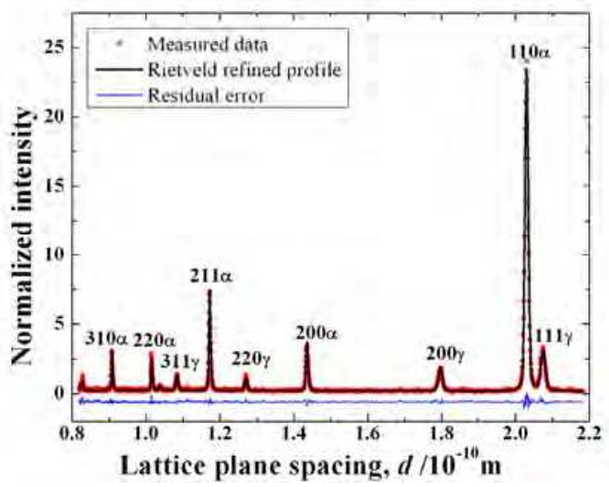

Fig. 8. Neutron diffraction spectrum of 3.6ks pre-tempered 17Ni-0.C martensite steel obtained at room temperature and its Rietveld refinement result taking all diffraction peaks measured into consideration. (Xu, 2008b)

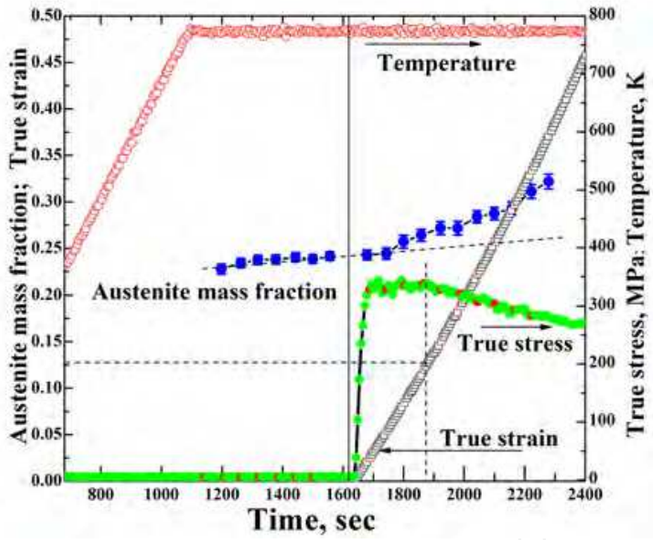

Fig. 9. Change in austenite fraction during 773K isothermal holding and warm compression.

4.2 Change in austenite diffraction spectra during warm compression

Fig.9 gives the changes in austenite fraction and true strain monitored with a high-temperature extensometer during warm compression as a function of time, showing that the austenite amount increases gradually with increasing compressive strain, *i.e.* from 24% at ε=0.0 to 32% at ε=0.33. Compared with the isothermal holding test, it is clear that the isothermal compression accelerates the austenite precipitation. In addition, the flow stress approaches the maximum value at a true strain about ε=0.13, and then gradually decreases.

Accordingly, the stress-strain curve is divided into two parts: (1) Region I, work hardening; (2) Region II, work softening.

Fig.10 compares the (111) diffraction peaks of austenite obtained in the axial direction at different loading steps during the warm compression at 873K. Though the austenite (111) peak intensity at ε=0.05 has almost equal to that at ε=0.0, the (111) lattice plane spacing at ε=0.05 (d_{111} =0.208428±0.000013 nm) is smaller than that at ε=0.0 (d_{111}^0 =0.208826±0.000007 nm). In other words, the lattice strain of austenite, $\varepsilon_{111} = (d_{111} - d_{111}^0) / d_{111}^0$, is about -1906×10-6, which is comparable with the elastic strain of the specimen estimated by $\varepsilon = \sigma / E$ =-1781×10-6 where the external stress σ is about 330MPa. Here the high-temperature Young's modulus E is taken as 185GPa (Sawada, 2005). That is to say, the (hkl) peak shifts of austenite related to the lattice strain are mostly due to the external stress.

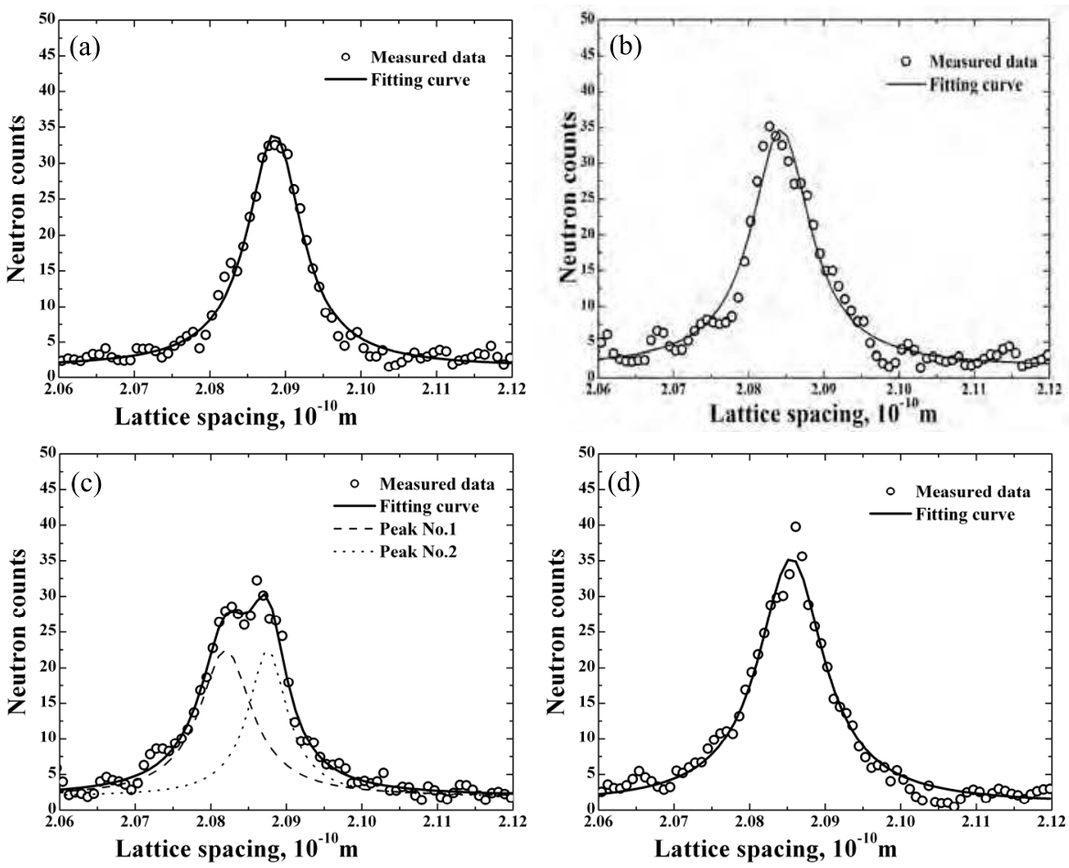

Fig. 10. Austenite (111) peaks and fitting results: (a) non-splitting, ε=0.0; (b) peak shift, ε=0.05; (c) peak splitting at ε=0.15; (d) disappearance of peak splitting at ε=0.33.

As the true strain increases to 0.15, the external stress increases only a little bit (see Fig.9), so that the amount of further peak shift is very limited. After this stage, the decreasing external stress with increasing true strain leads to a smaller peak shift in the opposite sense. On the other hand, the austenite (111) peak at ε=0.15 splits into two peaks with lower peak intensities (see Fig.10c). However, this peak splitting gradually disappears by ε=0.33, by

which stage there is again a single peak with a higher intensity. Considering the peak intensities of such neutron spectra were not strong, the third TOF profile function (Larson, 2004) was employed to fit the austenite (111) peaks. The splitting of austenite (111) peak suggests that newly precipitated austenite possesses lower carbon and nickel contents from those of the pre-existing austenite. Then, the chemical composition of austenite gradually becomes uniform with increasing compressive strain.

4.3 Change in ferrite diffraction spectra during warm compression

Fig.11 compares the (110) diffraction peaks of ferrite obtained in the axial direction at different loading steps at 773K. The (110) lattice plane spacing at ε=0.05 (d_{110}=0.203425±0.000007 nm) is smaller than that at ε=0.0 (d^0_{111}=0.203780±0.000007 nm). In other words, the lattice strain of ferrite, $\varepsilon_{110} = (d_{110} - d^0_{110}) / d^0_{110}$, is about -1742×10-6, lower than that of austenite ε_{111}. The *hkl*-specific elastic moduli E^K_{hkl}, calculated by the Kröner model, are 247.9 GPa for the austenite along the [111] direction and 225.5 GPa for the ferrite along the [110] direction (Hutchings, 2005), respectively. Therefore, the austenite is subject to a higher average phase stress than the ferrite matrix at the beginning of warm compression, *i.e.* the pre-existing austenite is harder than the ferrite matrix. In comparison with diffraction peaks obtained at ε=0.0, all (*hkl*) ferrite peaks show clear peak shifts at ε=0.05 due to the external stress about 330MPa. The ferrite (110) peak intensity decreases substantially and the ferrite (211) peak intensity increases a little. When the strain increases to ε=0.15, the ferrite (110) peak intensity decreases slowly but the ferrite (211) and (200) peak intensities decrease significantly.

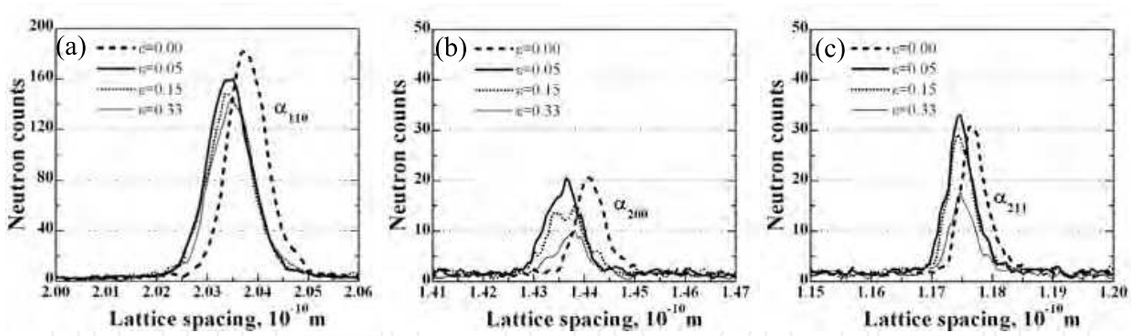

Fig. 11. Comparison of ferrite axial diffraction peaks of the 17Ni-0.2C steel at different compressive strains: (a) ferrite (110) peak; (b) ferrite (200) peak; (c) ferrite (211) peak. (Xu, 2008b)

Fig.12 shows the change in integrated intensities of different diffraction peaks with increasing of the compressive strain, obtained by single peak fitting of neutron spectra measured both in the axial and the radial directions of cylinder specimen. Before the compressive strain increases to 0.13, *i.e.* before the true stress reaches the maximum value, the ferrite (110) integrated intensity obtained in the axial direction decreases rapidly but that obtained in the radial direction decreases slowly. When the compressive strain is beyond ε=0.13, the decrease in ferrite (110) intensity in the axial direction becomes much slower while the decrease in the radial direction accelerates markedly. For the ferrite (200) and (211)

peaks, the integrated intensities obtained in the axial direction increase slowly before ε=0.13 and then decrease evidently beyond ε=0.13, but such data obtained in the radial direction show little change during the warm compression. Based on these changes in ferrite crystallographic orientation, the strain corresponding to the maximum true stress can be regarded as the onset strain for dynamic recrystallization of ferrite from martensite.

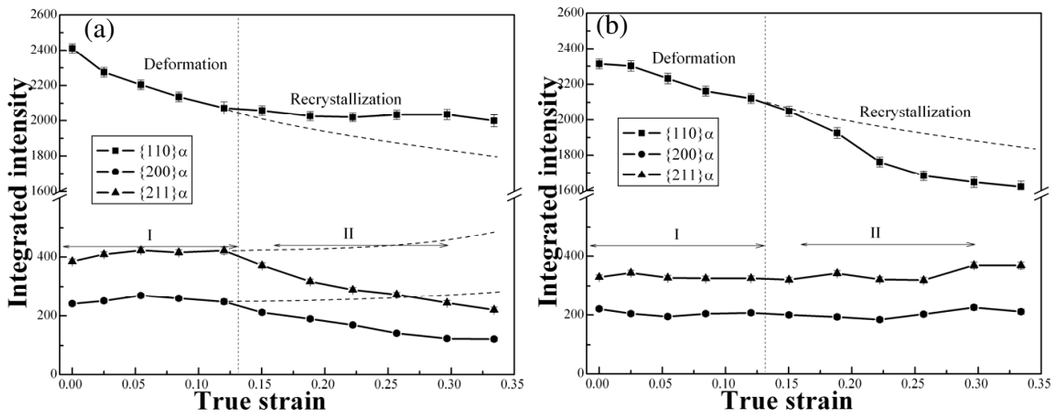

Fig. 12. Change in integrated intensity of ferrite in 17Ni-0.2C steel during warm compression: (a) obtained from the axial neutron spectra; (b) obtained from the radial neutron spectra. Regions I and II correspond to the ferrite deformation and the ferrite dynamic recrystallization, respectively. (Xu, 2008b)

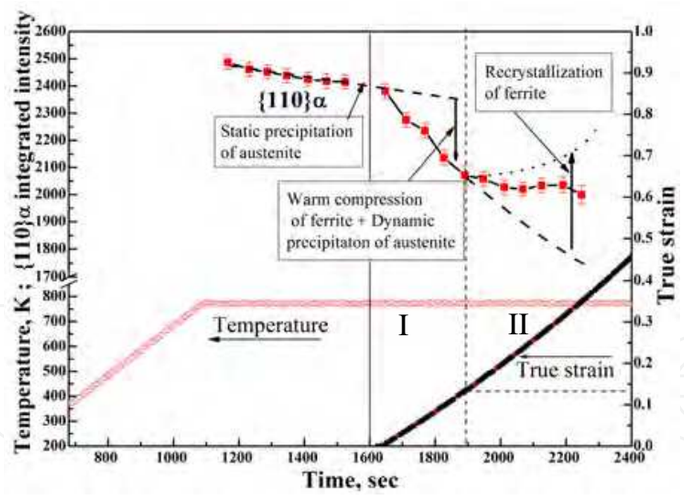

Fig. 13. Illustration for the microstructure evolution during isothermal holding and warm compression, based on the change in integrated intensity of ferrite (110) peak obtained in the axial direction.

Fig.13 illustrated the microstructure evolution based on the change in integrated intensity of ferrite (110) peak acquired in the axial direction during the isothermal holding and warm compession of 17Ni-0.2C martensite steel with 3.6ks prior tempering treatment. During the isothermal holding, the ferrite (110) integrated intensity decreases slowly due to the static precipitation of austenite. During the warm compression in the Region I, the warm compression

of ferrite and the dyanmic precipitation of austenite accelerate the reduction of the ferrite (110) integrated intesity and form a clear deviation from the change trend of ferrite (110) integrated intensity in during the isothermal holding; when the strain surpasses the critical strain 0.13, the compessed ferrite grains begins to recrystalize, which leads to an evident increase of ferrite (110) integraed intensity as marked by the dotted line if there is no other microstructure evolution. The co-existence of the ferrite recrystallization as marked by the dotted line and the ferrite deformation as marked by the dashed line (which is partially related to austenite precipitation) means that the so-called ferrite dyamic recrystallization really takes place. In other words, the microstructure evolution in the Region II is involved in the dyanamic ferrite recrystallization and the dynamic austenite precipitation, and their compitition effect is believed to result into the slow decrease in the ferrite (110) integrated intensity.

4.4 Effect of the existence of austenite grains on dynamic recrystallization of ferrite

Following the dynamic recrystallization, the flow stress decreases gradually to a stable stress. Since the external loading and the composition change in constituent phases both affect the lattice plane spacing, it is difficult to compare the lattice compressive strains directly during warm compression beyond ε=0.05. Considering that the plastic deformation changes the texture as described above, the texture indexes of the two constituent phases can be used to make an indirect comparison between the plastic strains of austenite and ferrite.

According to Bunge's definition (Bunge, 1982), the texture index J is a parameter to characterize the sharpness of the texture by the integral of the square of the texture function $f(g)$, without considering the details of the crystallographic orientation distribution:

$$J = \oint [f(g)]^2 \mathrm{d}g = \sum_{l,\mu,\nu} \frac{1}{2l+1} \left| C_l^{\mu\nu} \right|^2 \tag{2}$$

where l, μ and ν are the series expansion orders and $C_l^{\mu\nu}$ is the corresponding expansion coefficient. For a random texture, J=1.0 and for an ideal texture of single orientation, $J \rightarrow \infty$. Generally, heavier plastic deformation leads to sharper texture. In addition, the TOF neutron spectrum measurement covers a wide range of lattice plane spacings which is partially equivalent to measuring one reflection over a wide range of sample orientations. Therefore, the texture indexes calculated from the TOF neutron spectra by the GSAS software package (Larson, 2004) can be employed to compare the plastic strains of austenite and ferrite.

As shown in Fig.14, the texture indexes of the ferrite phase are evidently larger than those of austenite in both the axial and radial directions while the difference between the two directions is related to the details of the crystallographic orientation distribution. This suggests that the plastic deformation occurs preferentially in the ferrite matrix during warm compression.

The different peak shifts in Section 4.2 & Section 4.3 reveal that the austenite grains are harder than the ferrite grains. The texture index of the ferrite matrix is larger than that of austenite, suggesting that the plastic deformation occurs preferentially in the ferrite matrix. According to the related recrystallization literature (Doherty, 1997), the recrystallized ferrite grains nucleate preferentially in the heterogeneously deformed regions near large hard particles. Therefore, the existence of carbon-enriched austenite is able to accelerate the dynamic recrystallization in the ferrite matrix.

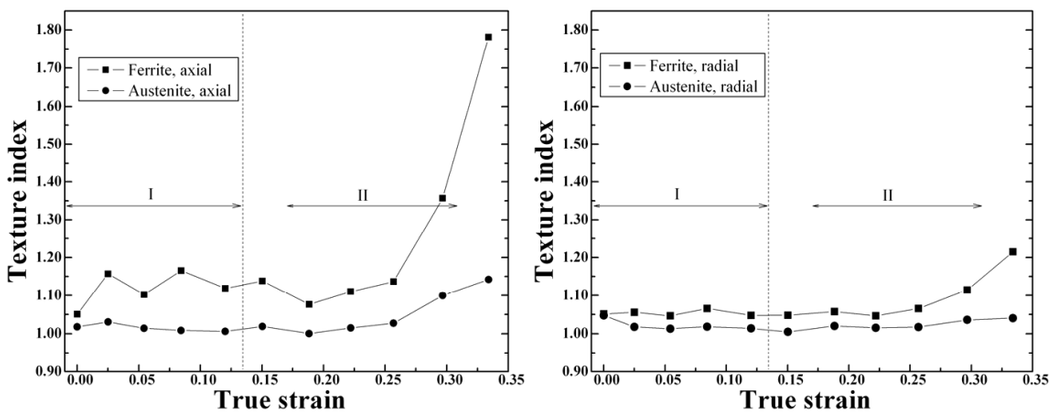

Fig. 14. Change in texture indexes of austenite and ferrite during warm compression: (a) obtained from the axial direction; (b) obtained from the radial direction. (Xu, 2008b)

The TOF neutron diffraction experiment helped us to understand the austenite precipitation and dynamic recrystallization behaviors of the 17Ni-0.2C martensite steel during isothermal warm compression after isothermal holding at 773K, and the main results were as follows: (1) the warm deformation at 773K accelerated the austenite precipitation in 17Ni-0.2C martensite steel. Splitting of the austenite (111) peak was found to occur and then disappear during warm compression. The splitting is ascribed to the different carbon concentrations in the dynamically precipitated austenite and the pre-existing austenite, and the disappearance of splitting is related to carbon homogenization at larger strain. (2) The austenite in the 17Ni-0.2C martensite steel is harder than the ferrite matrix at 773K. Heterogeneous deformation occurs preferentially in the ferrite matrix, leading to the acceleration of dynamic recrystallization.

5. Summary and future works

The low-carbon martensite steel and the high-nickel martensite steels have been warm compressed with and without prior tempering treatment to realize the microstructure refinement based on dynamic recrystallization at lower Zener-Hollomon parameter Z. Because of the lower critical strain for fully recrystallization compared with the warm deformation of ferrite or pearlite/ferrite, the warm deformatioin of martensite may be employed to the production of future ultrafine grained multiphase steels. The carbon addition promotes the formation of hard second phase particles such as cementite and austenite, which accelerates the ferrite recrystallization through the formation of local high strain regions near the hard particles during warm deformation.

Neutron diffraction has been applied as a powerful tool to investigate the microstructure evolutions of bulk materials during tensile/compressive deformation, heating/cooling and under other specific environmental conditions (te Velthuis, 1998; Tomota, 2005; Xu, 2006a; Xu, 2006b). Recently, TOF (*hkl*) multiple reflection spectra obtained by neutron diffraction have been analyzed to evaluate the crystallographic textures during forward and reverse diffusional phase transformations (Wenk, 2007) and the preferred orientations of ferrite and austenite in a 0.2C-2Mn steel before and after hot compression (Xu, 2009). The *in situ*

microstructure and texture evolution during thermomechical controlled process will be studied further in order to well optimize the multiphase microstructure (Xu, 2012).

6. Acknowledgments

The authors thank Dr. Y. Adachi at National Institute for Materials Science, Japan for his support on the TEM microstructure observation. They also appreciate Dr. E.C. Oliver at ISIS Facility, Rutherford Appleton Laboratory, United Kingdom for his support on the neutron diffraction.

7. References

Ameyama, K.; Matsumura, N. & Tokizane, M. (1988). Ultrafine Austenite Grains Obtained by Thermomechanical Processing in Low and Medium Carbon Steels. *Journal of the Japan Society for Heat Treatment*, Vol.28, no.4, pp.233-240, ISSN 0288-0490.

Bao, Y.Z.; Adachi, Y.; Toomine, Y.; Suzuki, T.; Xu, P.G. & Tomota, Y. (2005a). Dynamic Recrystallization Behavior in Martensite in 18Ni, 17Ni-0.2C and SM490 Steels. *Tetsu-to-Hagané* (Journal of the Iron and Steel Institute of Japan), Vol.91, pp. 602-608, ISSN 0021-1575.

Bao, Y.Z.; Adachi, Y.; Toomine, Y.; Xu, P.G.; Suzuki, T. & Tomota, Y. (2005b). Dynamic Recrystallization by Rapid Heating Followed by Compression for a 17Ni-0.2C Martensite Steel. *Scripta Materialia*, Vol.53, pp. 1471-1476, ISSN 1359-6462.

Bunge, H.J. (1982) *Texture Analysis in Materials Science*. Butterworth & Co., ISBN 0-408-10642-5, London, pp.88-98.

Chen, S.C.; Tomota, Y.; Shiota, Y.; Toomine, Y. & Kamiyama, T. (2006). Measurements of Volume Fraction and Carbon Concentration of the Retained Austenite by Neutron Diffraction. *Tetsu-to-Hagané* (Journal of the Iron and Steel Institute of Japan), Vol.92, pp.557-561, ISSN 0021-1575.

Doherty, R.D.; Hughes, D.A.; Humphreys, F.J.; Jonas, J.J.; Juul Jensen, D.; Kassner, M.E.; King, W.E.; McNelley, T.R.; McQueen H.J. & Rollett, A.D. (1997). Current issues in recrystallization: a review. *Materials Science and Engineering A*, Vol.238, pp.219-274, ISSN 0921-5093.

Dong, H. & Sun, X.J. (2006). Deformation induced ferrite transformation in low carbon steels. *Current Opinion in Solid State and Materials Science*, Vol.9, pp.269-276, ISSN 1359-0286.

Enomoto, M. & Furubayashi, E. (1977). A Crystallographic Study of Austenite Formation from Fe-Ni Martensite during Heating in Alpha-Gamma Region. *Transactions of the Japan Institute of Metals*, Vol.18, pp.817-824, ISSN 0021-4434.

Furuhara, T.; Yamaguchi, T.; Furimoto, S. & Maki, T. (2007). Formation of Ferrrite+Cementite microduplex structure by warm deformation in high carbon steels. *Material Science Forum*, Vol.539-543, pp.155-160, ISSN 0255-5476.

Glovre, G. & Selllers, C.M. (1973). Recovery and recrystallization during high temperature deformation of α-iron. *Metallurgical Transactions*, Vol.4, pp. 765-775, ISSN 0026-086X.

Hayashi, T.; Torizuka, S.; Mitsui, T.; Tsuzaki, K. & Nagai, K. (1999). Creation of low-carbon steel bars with fully fine ferrite grain structure through warm grooved rolling. *CAMP-ISIJ* (Current Advances in Materials and Processes), Vol.12, pp.385-388, ISSN 1882-8922.

Hayashi, T. & Nagai, K. (2002). Inprovement of strength-ductility balance for low carbon ultrafine-grained steel through strain hardening design. *Transactions of the Japan Society of Mechanical Engineers. A*, Vol.68, pp.1553-1558, ISSN 0387-5008.

Hutchings, M.T.; Withers, P.J.; Holden, T.M. & Lorentzen, T. (2005). *Introduction to the Characterization of Residual Stress by Neutron Diffraction*, ISBN 0-415-31000-8, Taylor & Francis, New York, pp.230-238.

Larson, A.C. & Von Dreele, R.B. (2004). General Structure Analysis System (GSAS), *Los Alamos National Laboratory Report.* LAUR 86-748, pp.147-148.

Li, J.H.; Xu, P.G.; Tomota, Y. & Adachi, Y. (2008) Dynamic Recrystallization Behavior in a Low-carbon Martensite Steel by Warm Compression. *ISIJ International*, Vol.48, no.7, pp.1008-1013, ISSN 1485-1664.

Maki, T.; Okaguchi, S. & Tamura, I. (1982). Dynamic recrystallization in ferritic stainless steel. Strength of metals and alloys (ICSMA 6) : Proceedings of the 6th International Conference, pp.529-534., ISBN 0080293255. Melbourne, Australia, 16-20 August 1982.

Maki, T.; Furuhara, T.; & Tsuzaki, K. (2001). Microstructure Development by Thermomechanical Processing in Duplex Stainless Steel. *ISIJ International*, Vol..41. pp. 571-579. ISSN 1485-1664.

Miller, R.L. (1972). Ultrafine-grained microstructures and mechanical properties of alloy steels. *Metallurgical Transactions*, Vol.3, pp.905-912, ISSN 0026-086X.

Moriyama, M.; Takaki, S. & Kawagoishi, N. (2001). Influence of Reversion Austenite on Fatigue Property of 350 ksi Grade 18Ni Maraging Steel. *Journal of the Japan Society for Heat Treatment*, Vol.41. pp.266-271, ISSN 0288-0490.

Najafi-Zadeh, A.; Jonas, J.J. & Yue, S. (1992). Grain refinement by dynamic recrystallization during the simulated warm-rolling of interstitial free steels. *Metallurgical Transactions A*, Vol.23, pp.2607-2617. ISSN 0360-2133.

Ohmori, A. ; Torizuka, S. ; Nagai, K. ; Yamada K. & Kogo, Y. (2002). Evolution of ultrafine-grained structure through large strain-high Z deformation in a low carbon steel. *Tetsu-to-Hagané* (Journal of the Iron and Steel Institute of Japan), Vol.88, no. 12, pp.857-864, ISSN 0021-1575.

Ohmori, A.; Torizuka, S.; Nagai, K.; Yamada, K. & Kogo, Y. (2004). Effect of Deformation Temperature and Strain Rate on Evolution of Ultrafine Grained Structure through Single-Pass Large-Strain Warm Deformation in a Low Carbon Steel. *Materials Transactions*, Vol.45, pp.2224-2231, ISSN 1345-9678.

Poorganji, B.; Miyamoto, G.; Maki, T. & Furuhara, T. (2008). Formation of ultrafine grained ferrite by warm deformation of lath martensite in low-alloy steels with different carbon content. *Scripta Materialia*, Vol.59, pp.279-281, ISSN 1359-6462.

Reed, R.C. & Root, J.H. (1998). Determination of the Temperature Dependence of the Lattice Parameters of Cementite by Neutron Diffraction. *Scripta Materialia*, Vol.38, pp.95-99. ISSN 1359-6462.

Sawada, K.; Ohba, T.; Kushima, H. and Kimura, K. (2005). Effect of microstructure on elastic property at high temperatures in ferritic heat resistant steels. *Materials Science and Engineering A*, Vol.394, pp.36-42, ISSN 0921-5093.

te Velthuis, S.G.E.; Root, J.H.; Sietsma, J.; Rekveldt, M.T. & van der Zwaag, S. (1998). The ferrite and austenite lattice parameters of Fe-Co and Fe-Cu binary alloys as a function of temperature. *Acta Materialia*. Vol.46, pp.5223-5228, ISSN 1359-6454.

Tomota, Y.; Suzuki, T.; Kanie, A.; Shiota, Y.; Uno, M.; Moriai, A.; Minakawa, N. & Morii, Y. (2005). In situ neutron diffraction of heavily drawn steel wires with ultra-high strength under tensile loading. *Acta Materialia*. Vol.53, pp.463-467, ISSN 1359-6454.

Tomota, Y.; Narui, A. & Tsuchida, N. (2008). Tensile behavior of fine-grained steels, *ISIJ International*, Vol.48, pp.1107-1113, ISSN 1485-1664.

Torizuka, S. (2005) Production of ultrafine-grained steel bar and plate by high Z-large strain deformation in ferrite region. *Ferrum* (Bulletin of The Iron and Steel Institute of Japan), Vol.10, no.3, pp.188-195, ISSN 1341-688X.

Tsuji, N.; Matsubara, Y.; Saito, Y. & Maki, T. (1998). Occurance of Dynamic Recrystallization in ferritic Iron. *Journal of the Japan Institute of Metals*, Vol.62, pp.967-976. ISSN 0021-4876.

Tsuji, N.; Okuno, S.; Koizumi, Y. & Minamino, Y. (2004). Toughness of Ultrafine Grained Ferritic Steels Fabricated by ARB and Annealing Process. *Materials Transactions*, Vol. 45, no.7, pp.2272-2281, ISSN 1345-9678.

Ueji, R.; Tsuji, N.; Minamino, Y.; & Koizumi, Y. (2002). Ultragrain refinement of plain low carbon steel by cold-rolling and annealing of martensite. *Acta Materialia*, Vol.50, pp.4177-4189, ISSN 1359-6454.

Wenk, H.R.; Huensche, I. & Kestens, L. (2007). In-Situ Observation of Texture Changes during Phase Transformations in Ultra-Low-Carbon Steel. *Metallurgical and Materials Transactions A*, Vol.38, pp.261-267, ISSN 1073-5623.

Xu, P.G.; Tomota, Y.; Lukas, P.; Muransky, O. & Adachi, Y. (2006a). Austenite-to-ferrite transformation in low alloy steels during thermomechanically controlled process studied by in situ neutron diffraction. *Materials Science and Engineering A*, Vol.435, pp.46-53, ISSN 0921-5093.

Xu, P.G. and Tomota, Y. (2006b). Progress in materials characterization technique based on in situ neutron diffraction. *Acta Metallurgica Sinica*, Vol.42, pp.681-688, ISSN 0412-1961.

Xu, P.G.; Li, J.H.; Tomota, Y. and Adachi, Y. (2007). Effect of Carbon Addition on Ultrafine Grained Microstructure Formation by Warm Compression for Fe-18Ni Alloys, *Materials Science Forum*, Vol.558-559, pp.601-606, ISSN 0255-5476.

Xu, P.G.; Li, J.H.; Tomota, Y. & Adachi, Y. (2008a). Effects of Volume Fraction and Carbon Concentration of Austenite on Formation of Ultrafine Grained Ferrite/Austenite Duplex Microstructure by Warm Compression, *ISIJ International*, Vol.48, no.11, pp.1609-1617, ISSN 1485-1664.

Xu, P.G.; Tomota, Y. & Oliver, E.C. (2008b). Dynamic Recrystallization and Dynamic Precipitation Behaviors of a 17Ni-0.2C Martensite Steel Studied by *In Situ* Neutron Diffraction, *ISIJ International*, Vol.48, no.11, pp.1618-1625. ISSN 1485-1664.

Xu, P.G.; Tomota,Y.; Suzuki, T.; Yonemura, M. & Oliver, E.C. (2009). In Situ TOF Neutron Diffraction for Isothermal Ferrite Transformation during Thermomechanically Controlled Process of Low Alloy Steel. *Netsu Shori* (Journal of the Japan Society for Heat Treatment), Vol.49. special issue, pp.470-473. ISSN 0288-0490.

Xu, P.G.; Tomota, Y.; Vogel, S.C.; Suzuki, T.; Yonemura, M. & Kamiyama, T. (2012) Transformation Strain and Texture Evolution during Diffusional Phase Transformation of Low Alloy Steels Studied by Neutron Diffraction, *Reviews on Advanced Materials Science*. Vol.33. (in press). ISSN 1605-8127.

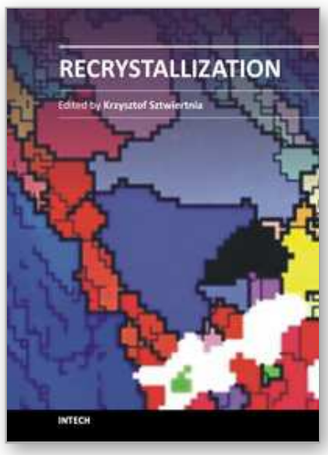

Recrystallization

Edited by Prof. Krzysztof Sztwiertnia

ISBN 978-953-51-0122-2
Hard cover, 464 pages
Publisher InTech
Published online 07, March, 2012
Published in print edition March, 2012

Recrystallization shows selected results obtained during the last few years by scientists who work on recrystallization-related issues. These scientists offer their knowledge from the perspective of a range of scientific disciplines, such as geology and metallurgy. The authors emphasize that the progress in this particular field of science is possible today thanks to the coordinated action of many research groups that work in materials science, chemistry, physics, geology, and other sciences. Thus, it is possible to perform a comprehensive analysis of the scientific problem. The analysis starts from the selection of appropriate techniques and methods of characterization. It is then combined with the development of new tools in diagnostics, and it ends with modeling of phenomena.

How to reference

In order to correctly reference this scholarly work, feel free to copy and paste the following:

Pingguang Xu and Yo Tomota (2012). Recrystallization Behavior During Warm Compression of Martensite Steels, Recrystallization, Prof. Krzysztof Sztwiertnia (Ed.), ISBN: 978-953-51-0122-2, InTech, Available from: http://www.intechopen.com/books/recrystallization/recrystallization-behavior-during-warm-compression-of-martensite-steels

INTECH
open science | open minds

InTech Europe
University Campus STeP Ri
Slavka Krautzeka 83/A
51000 Rijeka, Croatia
Phone: +385 (51) 770 447
Fax: +385 (51) 686 166
www.intechopen.com

InTech China
Unit 405, Office Block, Hotel Equatorial Shanghai
No.65, Yan An Road (West), Shanghai, 200040, China
中国上海市延安西路65号上海国际贵都大饭店办公楼405单元
Phone: +86-21-62489820
Fax: +86-21-62489821

IntechOpen